Pakistan Journal of Scientific Research (PJOSR)
ISSN (p): 0552-9050
Volume: 2, Number: 2, Pages: 10- 15, Year: 2022

Fault Detection of Electrical Machines Rolling Element and Prediction through AI

Mureed Hussain, Ali Suqrat, Muhammad Shaheer Amir Bajwa, and Kainat Fatima

Electrical Engineering Department, The University of Lahore, Lahore, 54000, Pakistan
Corresponding author: Mureed Hussain (e-mail: mureedsargana@gmail.com)

Received: 15/08/2022, Revised: 20/11/2022, Accepted: 10/12/2022

***Abstract*— The research examines how Artificial Intelligence (AI) and machine learning can identify a minor rolling element problem (hole and scratch). Keeping track of a machine's health makes it possible to spot problems before they become costly, unscheduled production process shutdowns. In the study, a multi-stage decision mechanism was built using the convolution neural network (CNN) model.**

***Keywords*— rolling element fault, ANN, Kurtosis, MATLAB, dataset**

I. INTRODUCTION

In most industrial environments, electrical machines (EM) are powered by mechanical systems. Continuous monitoring (CM) and early discovery of minor issues are essential for maintaining EM performance. Keeping track of a machine's health makes it possible to spot problems before they become costly, unscheduled production process shutdowns. Machine current signature analysis, often known as MCSA, has become a well-liked approach to condition-based maintenance. The MFPT Challenge data includes data collected from machines operating under various failure scenarios. Each data set consists of four critical frequencies that each reflect a different problem location, an acceleration signal ("gs"), a sampling rate ("sr"), a shaft speed ("rate"), and a load weight ("load"). The system was run at four different speeds for a brand-new rolling element with purposely induced local flaws of varied sizes [1]. Figure 1 hardware configuration.

Figure 1: Complete working setup.

II. BALL BEARING FUNDAMENTALS

A. The Fault of Ball Bearing

Ball bearing failure is one of the primary causes of rotating machine failure. The vibration response to various ball bearing issues is measured and studied. The specific faults are a break in the outer race, an inner race with a rough surface, and corrosion pitting in the balls. Ball bearing failure is one of the primary causes of rotating machine failure. So, accurate diagnosis and detection of mechanical ball-bearing faults are crucial for safe operation. The test rig consists of a high-speed rotor supported by rolling bearings. The vibration response to various ball bearing issues is measured and studied. The specific faults are a break in the outer race, an inner race with a rough surface, and corrosion pitting in the balls. Statistical techniques are used to extract characteristics and reduce the dimensionality of the original vibration information. When a bearing malfunctions, it typically results in the failure of a machine shaft and the breakdown of the apparatus. A bearing fails when it does not function or last as planned. Failure of a bearing has significant consequences for your facility [2]. A specific type of rolling element bearing called a ball bearing uses balls to maintain the distance between the bearing races. The primary purposes of a ball bearing are to support radial and axial loads and reduce rotational friction.

When the inner race flaw is close to the device's top, the machine strikes the balls more gently. The repeated modification of the impact forces is known as amplitude modulation, producing the 1x sidebands—inner fault bearing of Fig. 2.

Figure 2: Inner race defect.

B. Outer Race Fault

The distinguishing features of the spectrum are the outer race failure frequency harmonic peaks, shown in Fig.3.

Figure 3: Outer race defect.

C. Four Fault Frequencies

Ball pass frequency, outer race (BPFO) is given by

$$BPFO = \frac{nf_r}{2}(1 - \frac{d}{D}\cos\varphi) \quad (1)$$

$$BPFI = \frac{nf_r}{2}(1 + \frac{d}{D}\cos\varphi) \quad (2)$$

$$FTF = \frac{f_r}{2}(1 - \frac{d}{D}\cos\varphi) \quad (3)$$

$$BSF = \frac{D}{2d}[1 - \left(\frac{d}{D}\cos\varphi\right)^2] \quad (4)$$

III. Method to Diagnose the Ball Bearing Fault

This section presents the results, computer simulations, and mathematical elaborations. Starting with an explanation of the definitions of a keratogram and a spectrum kurtosis. Based on the mathematical modelling, the suggested structure is numerically simulated using MATLAB software. The results are shown and thoroughly described when the complete simulation is presented. A Diagram of a block is shown in Fig. 4.

Figure 4: Process flow chart.

A. Envelope Spectrum Analysis

Abbreviations and acronyms should be defined the first time they are used in the text, even if they have already been defined in the abstract. Acronyms like IEEE, SI, MKS, CGS, sc, dc, and rms do not need to be defined. Avoid using acronyms in the title or headings, if at all possible.

B. Kurtosis Analysis

A kurtosis graph and spectral Kurtosis are used to determine Kurtosis locally within frequency bands. Using these resources effectively, the frequency band with the highest Kurtosis (or signal-to-noise ratio) may be found [3]. After determining the frequency range with the highest Kurtosis, a bandpass filter may be added to the raw signal to produce a more impulsive signal for envelope spectrum analysis.

C. CNN

The categorization of the scalograms will subsequently be carried out using a fine-tuned SqueezeNet convolutional neural network. As a result of being trained on more than a million pictures, SqueezeNet has acquired rich feature representations. Transfer learning is commonly used in deep learning applications. For new tasks, a pretrained network can serve as a starting point. Transfer learning often speeds up and simplifies network optimization compared to random data training. After resetting to zero weights [4], Fewer training photographs may allow for quick transmission of acquired traits. After loading, view the SqueezeNet network.

IV. Simulation Results

The completed text alteration prepares the document for the template. Now you can generate a copy of the file and then name your paper using the convention advised by your conference. Then import your text file, highlighting each component of the newly created file. Once your document is finished, style it using the scroll-down window to the left of the MS Word Formatting toolbar.

As part of our senior project, we created a system that can detect and predict a rolling machine's bearing issue called Electrical Machines Rolling Element Issue Detection and Prediction using Artificial Intelligence. Our building system is based on artificial intelligence.

A. Case I:

a) Inner Envelop Spectrum

using the envelope spectrum analysis technique on the data of observed bearing acceleration.

Visualize the raw time domain data from the MFPT dataset for an inner race failure signal. Figure 5 depicts a graph between bearing acceleration and time. Figure 6 shows the spikes resulting from rolling elements slamming into local faults at inner races or from rolling element faults attacking inner races. To see the frequency response at BPFI and its first few harmonics in greater detail, now increase the low-frequency region of the raw signal's power spectrum. There is no observable pattern at BPFI and its harmonics [4].

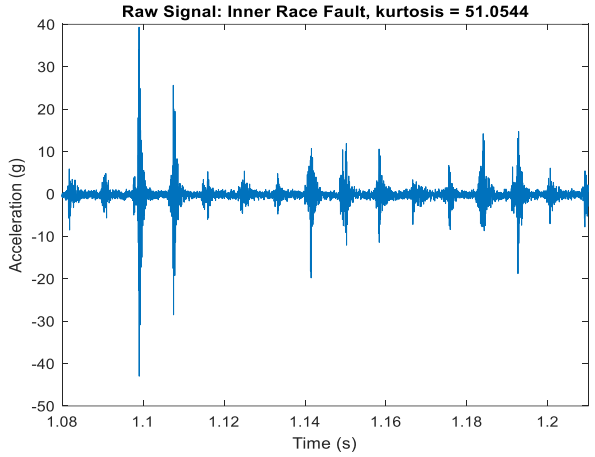

Figure 5: Enveloped spectrum of inner race fault in the time domain.

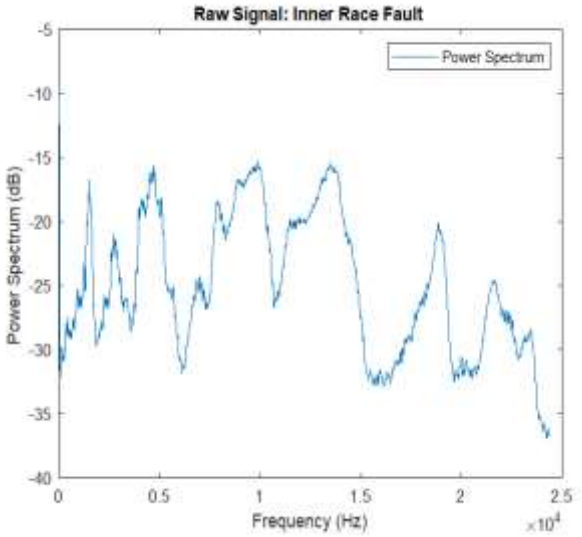

Figure 6: Enveloped spectrum of inner race fault in the frequency domain.

Next, to evaluate the envelope spectrum, look at Fig. 7 for the frequency response at BPFI and its harmonics.

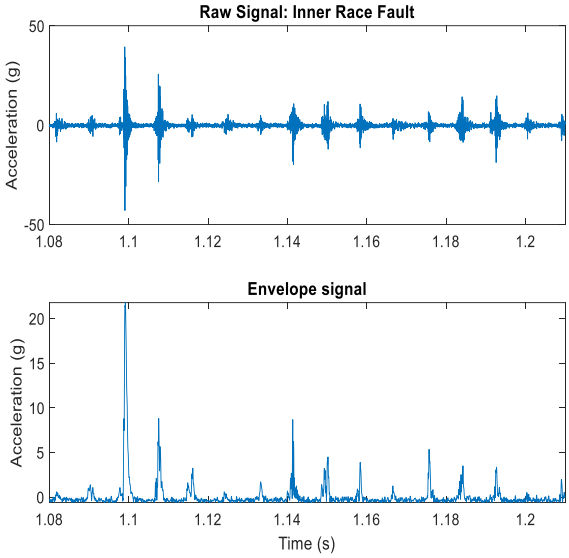

Figure 7: Signal modulation for a given frequency (time domain).

b) Inner Kurtosis Analysis:

Kurtosis is calculated locally within frequency bands using a kurtosis graph and spectral Kurtosis. They are effective methods for identifying the frequency band with the maximum Kurtosis (or the highest signal-to-noise ratio).

The raw signal can be subjected to a bandpass filter to produce a more impulsive signal for envelope spectrum analysis and the spectral Kurtosis shown in Fig.9 after determining the frequency band with the highest Kurtosis.

The largest Kurtosis is found in the frequency band with a bandwidth of 1.0172 kHz and a central frequency of 13.7329 kHz, according to the kurtogram [5]. Figure 8. shows an inner flaw.

To compute the spectral Kurtosis, utilize the best window length indicated by the kurtogram.

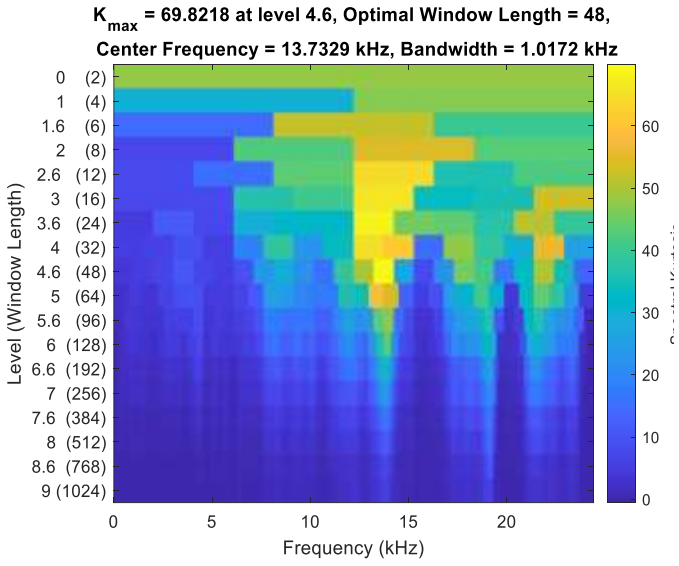

Figure 8: Inner race fault kurtogram.

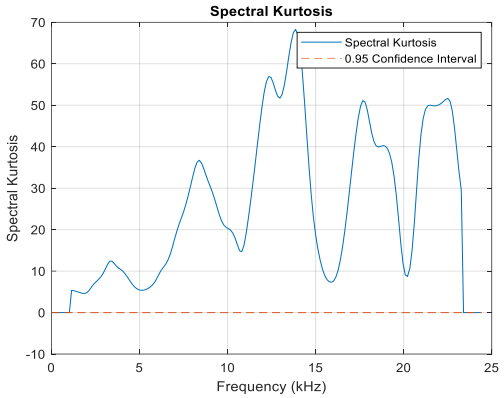

Figure 9: Spectral kurtosis of the optimal window length.

Compute the spectrogram and place the spectral Kurtosis on the side to see the frequency band on the graph. [6]. To understand spectral Kurtosis from a different perspective, large values of the spectral Kurtosis signify a significant variation in power at the corresponding frequency, making spectral Kurtosis a helpful tool for identifying nonstationary signal components.

The modulated amplitude of the inner race fault may be recovered, and the Kurtosis can be improved by applying a bandpass filter to the signal with the specified centre frequency and bandwidth [2]. Figures 10 and 11 demonstrate an inner race defect and an envelope, respectively.

After bandpass filtering, the kurtosis value is shown to have risen. The envelope signal will now be shown in the frequency domain.

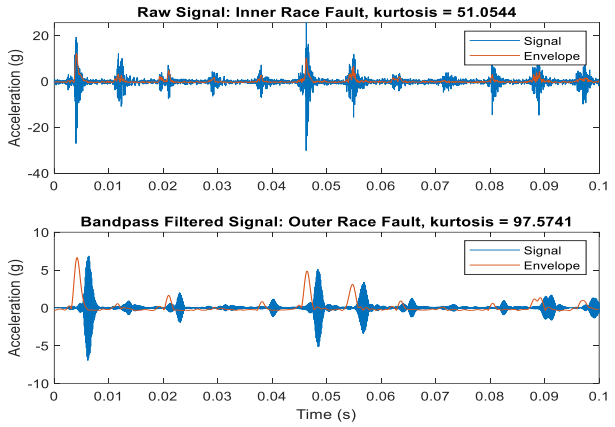

Figure 10: Retrieved inner race fault from the filtered signal.

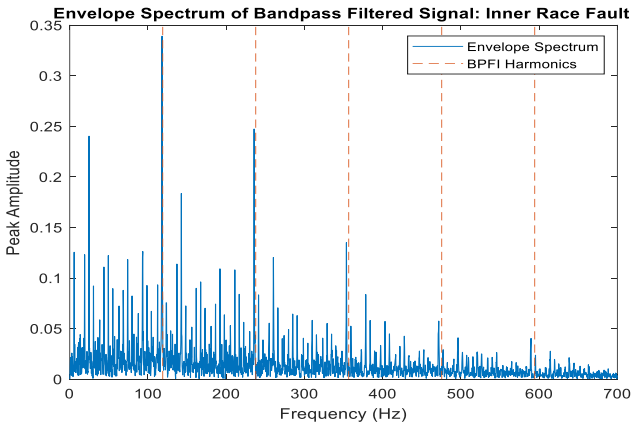

Figure 11: Inner race fault envelope signal in frequency domain.

B. Case II:

a) Inner Envelop Spectrum:

Using the envelope spectrum analysis technique on the data of observed bearing acceleration.

See the vibration dataset's raw time domain data for an inner race failure signal. Figure 27 depicts a graph between bearing acceleration and time when rolling elements clash with local faults, as shown in Fig.13 [7].

Watch the raw data in the current frequency range. To highlight the spectrum to more closely analyze the frequency response at BPFI and its first few harmonics [7].

At BPFI and its harmonics, no discernible pattern is seen. The raw signal's frequency analysis does not yield any relevant diagnostic data [7], and Fig. 12 kurtosis illustrates this.

b) Inner Kurtosis Analysis:

A kurtosis graph and spectral Kurtosis are used to determine Kurtosis locally within frequency bands. Using these tools, the frequency band with the highest Kurtosis (signal-to-noise ratio) may be found effectively [8]. A frequency band is seen in Fig. 15.

To get a better response for the envelope detection, we used the best technique, and the results are in Fig 14.

The largest Kurtosis, with a value of 704.33, is found in the frequency band with a bandwidth of 0.763 kHz and a centre frequency of 5.722 kHz, as shown by the Kurtogram. Utilize the optimal window length suggested by the Kurtogram to calculate the spectral Kurtosis.

Fig. 12 illustrates the resulting acceleration spikes for the rolling collision with the internal races or when the locality hits the internal races and clashes with each other.

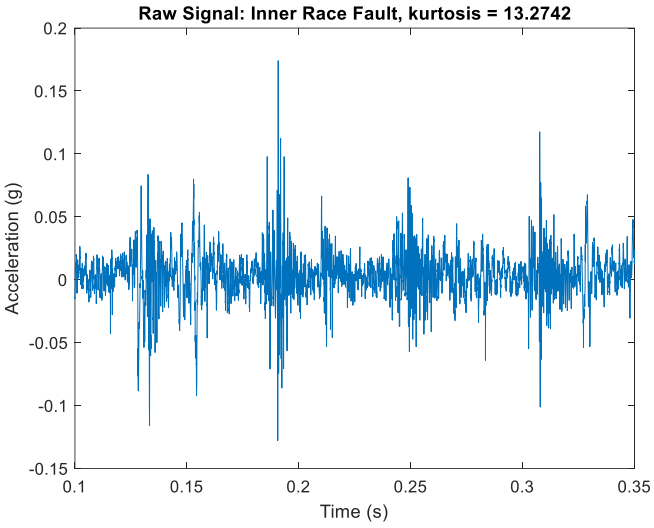

Figure 12: Kertosis spectrum of inner race fault in the time domain.

To further evaluate and visualize the analysis of the Kurtosis, which may also be interpreted as high spectral kurtosis values implying a considerable change in power at the corresponding frequency [8], is a useful technique for locating nonstationary signal components.

The signal can be bandpass filtered using the advised centre spectrum, improving the Kurtosis and extracting the signal amplitude. The kurtosis value is seen to have increased following bandpass filtering. Now think about the inner fault in Figs. 16 and 17 and the frequency domain envelope signal [8].

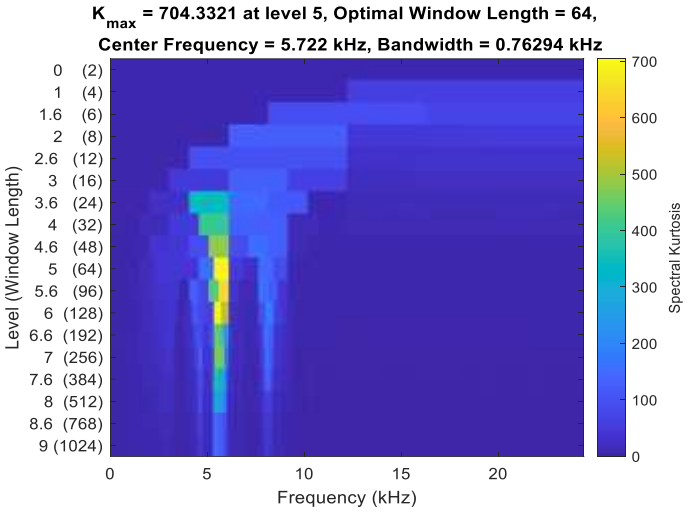

Figure 13: Inner race fault Kurtogram.

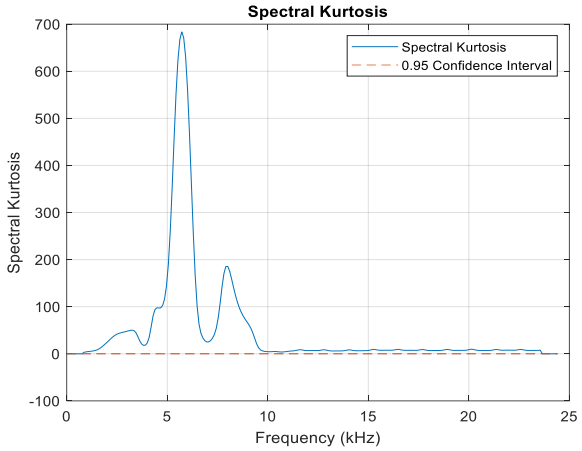

Figure 14: Spectral Kurtosis of the optimal window length.

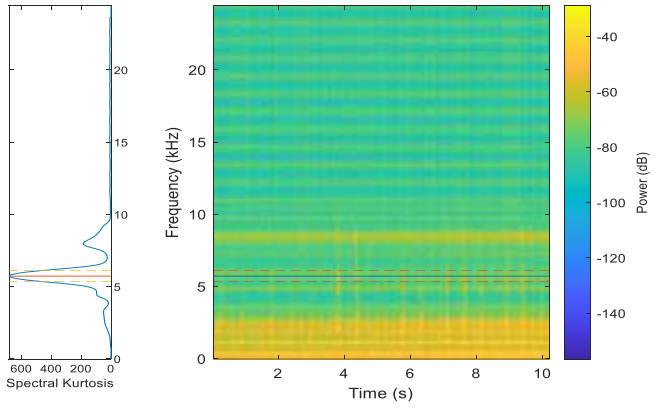

Figure 15: Visualizing the frequency band on a spectrogram.

C. By passband filtering, the signal with some fluctuations having some spectrum given by the Kurtogram and the spectral analysis for the envelope may get the results of fault signature at the passband filtering integral and its other harmonics. This has been suggested and reported in [8].

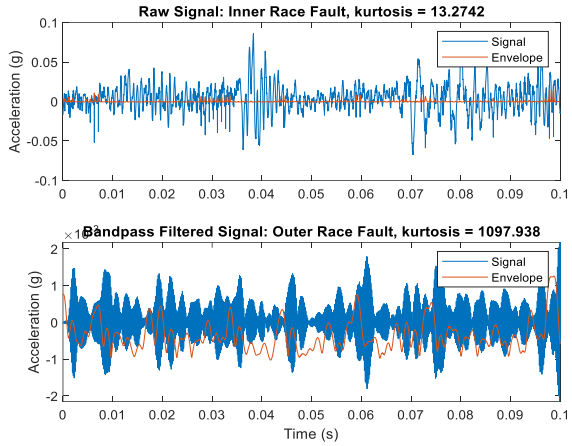

Figure 16: Retrieved inner race fault from the filtered signal.

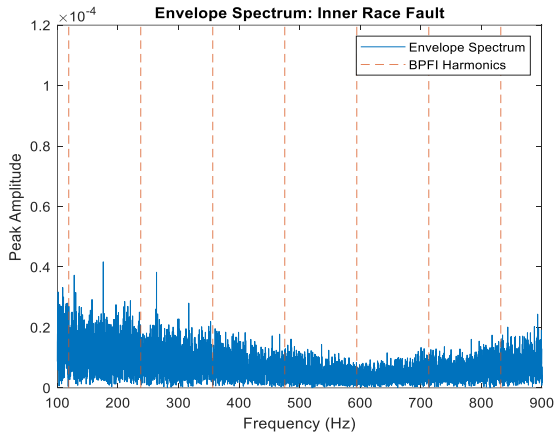

Figure 17: Inner race fault envelope signal in the frequency domain.

D. *CNN Case I Results*

a) *Algorithm Training Session*

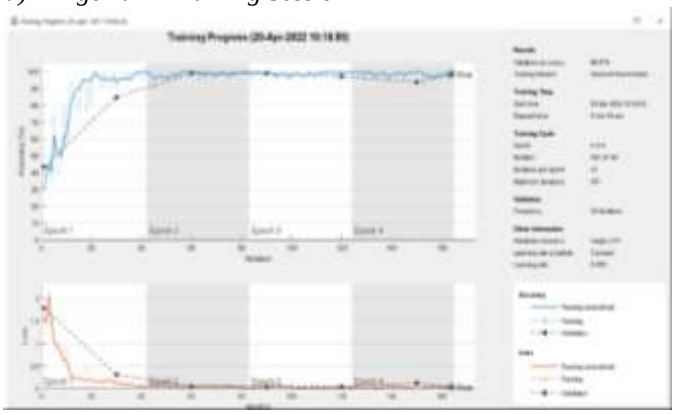

Figure 18: Algorithm training process.

b) The network's new and transferred layers should be trained. Train Network automatically uses a GPU if you have Parallel Computing ToolboxTM and supported GPU hardware. For information on supported devices, see GPU Support by Release (Parallel Computing Toolbox). Otherwise, the railway Network uses a CPU. The training choices and methodology depicted in fig. 18's execution environment parameter has the name-value combination "Execution Environment."

c) *Algorithm Testing*

d) Check the trained network's accuracy using the bearing signals in the "Bearing Readings /test data" folder. The training and test data need to go through the same processing processes. Create an ensemble data storage file so you may preserve the bearing vibration signals in the test folder. From 1-D signals, generate 2-D scalograms. Create an image data store to save the sample pictures. Utilize the trained network to categorize the stored test picture data.

e) *Accuracy*

We estimate the convolution neural network algorithm's prediction accuracy to be 98.07% after training and testing.

f) *Testing Session*

Make a confusing matrix. This demonstrates that deep learning may be valuable for recognizing distinct failure types in rolling element bearings, even with small data. As seen in Fig. 19, utilizing a deep learning strategy reduces the time required for feature engineering compared to a conventional method.

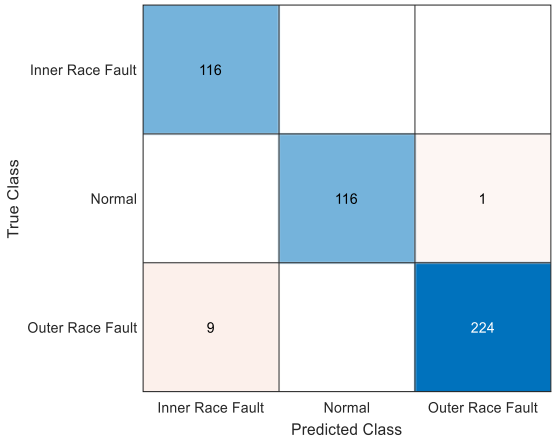

Figure 19: Prediction results using a confusion matrix.

E. *CNN Case II Results*

a) *Algorithm Training Session*

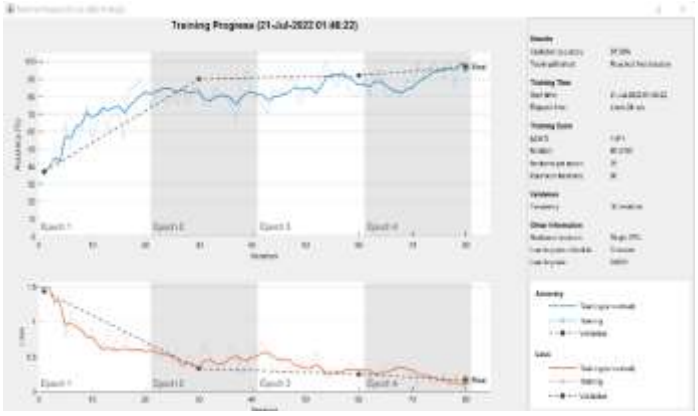

Figure 20: Algorithm training process.

The network's new and transferred layers should be trained. Another technique to characterize the execution environment is through the name-value parameter 'Execution Environment' of the training options [9].

b) *Algorithm Testing*

Check the trained network's accuracy using the bearing signals in the "Bearing Readings/test data" folder. The

training and test data need to go through the same processing processes. Create an ensemble data storage file so you may preserve the bearing vibration signals in the test folder. From 1-D signals, generate 2-D scalograms. To store the test photos, create an image data store. Use the trained network to classify the test picture data storage.

c) Accuracy

A convolution neural network was used to train and test the algorithm, and we estimated that the prediction accuracy was around 91%.

d) Testing Session

Make a confusing matrix. This demonstrates that deep learning may be valuable for recognizing distinct failure types in rolling element bearings, even with small data. As seen in fig.21, a deep learning strategy reduces the time required for feature engineering and prediction compared to a conventional approach.

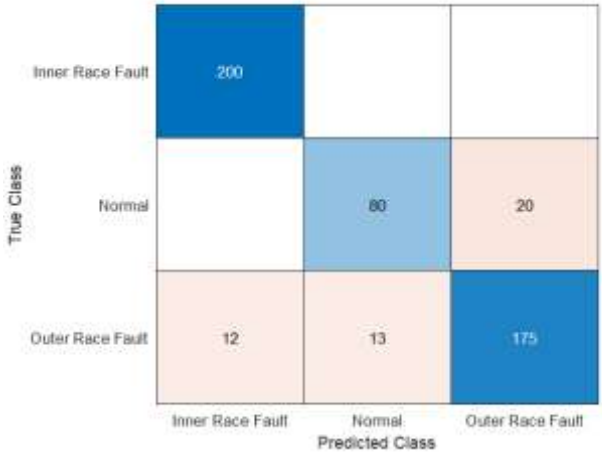

Figure 21: Prediction results using a confusion matrix.

FUNDING STATEMENT

The authors declare they have no conflicts of interest to report regarding the present study.

CONFLICT OF INTEREST

The Authors declare that they have no conflicts of interest to report regarding the present study.

V. CONCLUSION

As part of our senior project, we created a system that can detect and predict a rolling machine's bearing issue called Electrical Machines Rolling Element Issue Detection and Prediction using Artificial Intelligence. Our building system is based on artificial intelligence. When considering the temporal domain, we can see that the inner defect caused a distortion (a time-domain graph displays how a signal evolves). Because the findings were incorrect in the temporal domain, we did not acquire the information we needed for the outer defect and the bearing's normal condition. We can see that in the frequency domain, the frequency tells how the problem happened regarding time. The BPFIO equation describes how faults emerge at specific frequencies and during predetermined periods. When we apply Kurtosis, we see that while several frequencies are present in the kurtosis situation, a flaw only manifests on one specific frequency. While some frequencies have low values, those with high values can be used to detect malfunctions. We employ a CNN for flaw detection. In 80% of the situations, we test and train using the data we obtain. After that, the remaining 20% of the data is trained. Finally, we found that our method could be utilized to find both internal and external flaws.

REFERENCES

[1] A. Boudiaf, A. Moussaoui, A. Dahane, and I. Atoui, "A Comparative Study of Various Methods of Bearing Faults Diagnosis Using the Case Western Reserve University Data," *J. Fail. Anal. Prev.*, vol. 16, no. 2, pp. 271–284, Apr. 2016.

[2] S. Zhang, S. Zhang, B. Wang, and T. G. Habetler, "Machine Learning and Deep Learning Algorithms for Bearing Fault Diagnostics -- A Comprehensive Review," *IEEE Access*, vol. 8, pp. 29857–29881, 2020.

[3] S. Y. Li and K. R. Gu, "Smart fault-detection machine for ball-bearing system with chaotic mapping strategy," *Sensors*, vol. 19, no. 9, May 2019

[4] "Case Western Reserve University Bearing Data Center." [Online]. Available: https://csegroups.case.edu/bearingdatacenter/home. [Accessed: 22-Dec-2019].

[5] R. N. Bell, D. W. McWilliams, P. O'Donnell, C. Singh, and S. J. Wells, "Report of Large Motor Reliability Survey of Industrial and Commercial Installations, Part I," *IEEE Trans. Ind. Appl.*, vol. IA-21, no. 4, pp. 853–864, 1985.

[6] R. N. Bell, C. R. Heising, P. O'Donnell, S. J. Wells, and C. Singh, "Report of Large Motor Reliability Survey of Industrial and Commercial Installations, Part II," *IEEE Trans. Ind. Appl.*, vol. IA-21, no. 4, pp. 865–872, 1985.

[7]] W. Huang, J. Cheng, and Y. Yang, "Rolling bearing fault diagnosis and performance degradation assessment under variable operation conditions based on nuisance attribute projection," *Mech. Syst. Signal Process.*, vol. 114, pp. 165–188, Jan. 2019.

[8] M. S. Safizadeh and S. K. Latifi, "Using multi-sensor data fusion for vibration fault diagnosis of rolling element bearings by accelerometer and load cell," *Inf. Fusion*, vol. 18, no. 1, pp. 1–8, Jul. 2014.

[9] R. A. Patel and B. R. Bhalja, "Condition Monitoring and Fault Diagnosis of Induction Motor Using Support Vector Machine," *Electr. Power Components Syst.*, vol. 44, no. 6, pp. 683–692, Apr. 2016.